A Motion Induced Passive Infrared (PIR) Sensor for Stationary Human Occupancy Detection

Jack Andrews
Electrical and Computer Engineering Department
Oakland University
Rochester, MI, USA
jackandrews@oakland.edu

Meghana Kowsika
Electrical Engineering and Computer Science Department
University of Michigan
Ann Arbor, MI, USA
mkowsika@umich.edu

Asad Vakil
Electrical and Computer Engineering Department
Oakland University
Rochester, MI, USA
avakil@oakland.edu

Jia Li
Electrical and Computer Engineering Department
Oakland University
Rochester, MI, USA
li4@oakland.edu

***Abstract*—Passive Infrared (PIR) sensors are commonly used in indoor applications to detect human presence. PIR sensors detect human presence by detecting the change in infrared radiation across the polarity of the sensor. Due to this, PIR sensors are unable to accurately detect stationary human subjects, which results in false negatives. In the pursuit of creating a low-cost solution for detecting stationary occupants in a closed space, the novel approach to mount a PIR sensor on a moving platform was developed (MI-PIR). This approach was developed for the system to artificially induce the motion that is necessary for stationary human detection. Utilizing the raw analog output of the PIR sensor and an artificial neural network (ANN), the closed space was accurately classified for room occupancy, the number of occupants, the approximate location of the human targets, and the differentiation of targets. This novel approach provides the advantages of a utilizing a single PIR sensor for human presence detection, while eliminating the major known drawback to this type of sensor. Scanning the room using a PIR sensor also allows for an expanded field of view (FoV) and a simpler deployment, in comparison to other approaches using a PIR sensor. Finally, MI-PIR expands the functionalities of PIR sensors by using an ANN to detect various other occupancy parameters. The experimental results show that the system can detect room classification with 99% accuracy, 91% accuracy in occupancy count estimation, 93% accuracy in relative location prediction, and 93% accuracy in human target differentiation. These results show promise for an application of tracking and monitoring an at-risk patient in an indoor setting.**

Keywords—PIR sensor, artificial neural network (ANN), human detection, stationary occupancy

I. INTRODUCTION

Passive infrared (PIR) sensors have been used for human detection in various applications including smart homes [1], [2], smart cities [3], and biomedical applications including resting heart rate estimation [4] and epileptic seizure detection [5]. PIR sensors are popular due to their low-cost, low-complexity, and noninvasive nature with respect to the end user. PIR sensors detect human presence by having two or, in some cases, four pyroelectric elements wired in parallel. When one of the elements views more infrared radiation than the other, the PIR sensor will be triggered by this change in infrared radiation. During ambient conditions, each of the pyroelectric elements views the same infrared radiation and with no change between the elements, there is no triggering of human movement. As a result, when no human movement is detected in the field of view (FoV) of the PIR sensor, the output will be an unoccupied state, leading to false negatives. This major known drawback to PIR sensors limits the potential applications of PIR sensors. PIR sensors provide many advantages that lead them to be deployed in a number of environments; however, many applications require sensor fusion deployment to overcome the disadvantage of the lack of reliable stationary occupancy detection.

Human presence detection in an indoor environment is a popular research topic. Various sensor modalities have been chosen for deployment in numerous indoor human presence applications. Camera modalities have been deployed for human presence and associated parameters in an indoor environment, yet their invasive nature is the common reason for reluctance in utilizing this technology in domestic applications. Obtaining reliable accuracy is negated by these privacy concerns and the high computing power needed to handle image data. Wearable devices have been used for human presence detection, occupancy count, location prediction, and human target differentiation. Wearable devices provide a level of discomfort to the user that negates the high level of accuracy of the wearable device. Wearable devices include modalities such as radio frequency identification (RFID) tags and smart watches. Other approaches function properly, but come with higher costs than a PIR. These approaches include ultrasonic sensors, radio frequency (RF) based localization systems, and localization systems that equip active beacons. Thus, PIR sensors become a logical solution to indoor human presence, as they are non-invasive and low-cost, especially in comparison to the sensor modalities mentioned above.

There are many aspects of stationary human target detection with a PIR sensor that need to be further researched. Existing literature applies a common method in order to overcome this issue. In [6], this group provided the initial promise of using a PIR sensor to detect stationary occupants. The system was based on an optical shutter that periodically chops the thermal heat of the human body. Their design achieved 100% accuracy through analysis of maximum sensing distance with a FoV of 110 degrees. No room occupancy parameters were addressed in this work. In [7-8], this group has published three works on their system that detects stationary human targets with a single PIR

978-1-7281-0244-3/20/$31.00 ©2020 IEEE

Authorized licensed use limited to: OAKLAND UNIVERSITY. Downloaded on August 20,2020 at 14:47:54 UTC from IEEE Xplore. Restrictions apply.

sensor. Each of their respective papers have progressed their previous design, by adding more functionalities and reducing the power consumption of their design. Their design is similar to [6] with an optical shutter that periodically chops the FoV of their single PIR sensor. This group was also successful at stationary human detection with a FoV of 93 degrees in [8]. Also in [8], the group achieved a 97% accuracy in room classification during a 31 hour experiment.

Both designs developed modules to optically shutter a PIR sensor for stationary presence detection. Their respective modules are dependent on the Fresnel lens of the PIR sensor for FoV and are mechanically complex solutions to the problem. Neither of the groups addressed occupancy parameters such as occupancy count estimation, relative location prediction, or human target differentiation in their work.

In the effort to combine the low-cost, non-invasive, and passive capabilities of the PIR sensor with a simple design to detect stationary occupants, we developed a system that shows promise in this area. To the best of our knowledge, our design is the first of its kind. Our design works by inducing the motion needed for stationary human detection. By rotating a single PIR sensor on top of a robotic actuator in a constant, periodic cycle, a closed office space is scanned. With the combined technology of an artificial neural network (ANN), human presence was accurately detected. This novel motion induced approach is coined MI-PIR, and has provided accurate detection in the four occupancy parameters in a closed office space. MI-PIR allows for a greater FoV, where the entire office space can be scanned in a relatively short amount of time. Thus, MI-PIR is a novel approach for stationary human presence detection using a single PIR sensor and deep learning.

Overall, the contributions of this paper are as follows. We designed a novel approach for stationary human occupancy detection utilizing a single PIR sensor. This novel design provides advantages in comparison to similar works in that the FoV is expanded with MI-PIR due to the scanning nature of the design and the mechanical complexity is lowered. Finally, we expand the capabilities of a PIR sensor with the pairing of an ANN by accurately detecting the four occupancy parameters.

The four occupancy parameters include room classification, occupancy count estimation, relative location prediction, and human target differentiation. Room classification refers to an office space being occupied or unoccupied. An occupied state involves at least one human subject present in the room, whereas an unoccupied scenario involves no human subjects present. Occupancy count estimation classifies the number of human subjects present in the office space from zero being unoccupied to three individuals present. Relative location prediction classifies the location of human subjects in the office space, where the room is segmented into six possible locations, with a zero label indicating an unoccupied state. Finally, human target differentiation refers to differentiating human subjects based on the output of the PIR sensor. These labels can include unoccupied, one subject, or many subjects present.

The rest of the paper is organized as follows. Section II describes MI-PIR's novel design, including the hardware and the ANN. Section III examines the experimental portion of the work, including the data collection process. Section IV identifies the data analysis, providing evidence for the high accuracy obtained from the ANN. Section V is the results and discussion portion of the work. Finally, Section VI will provide the conclusions for the paper.

II. MI-PIR DESIGN

MI-PIR is composed of a single PIR sensor, a robotic actuator, a thermal insulator, a microcontroller, a PC, and an ANN for learning purposes. The hardware of MI-PIR will be discussed first and then the software architecture of the ANN will be presented.

A. Hardware

MI-PIR is based on a single PIR sensor system. The PIR sensor chosen for this application was the Panasonic AMN 24412 sensor, shown in Fig. 1. This sensor model was selected due to the device's analog output capability. More common PIR sensors on the market do not have analog output capability, and are dependent on their own threshold to determine if there is human presence. A digital PIR sensor would not function properly for MI-PIR, as the determined threshold would present false positives by all elements of the office space while in motion. This is due to the fact that everything above the absolute temperature emits some level of infrared radiation, with generally the greater the temperature, the more infrared radiation produced. Moreover, this PIR sensor has a 10 meter maximum detection distance, 110 degree vertical range, and a 93 degree horizontal range when applied in the traditional sense. The PIR sensor is wired to an Elegoo Uno R3 microcontroller for real-time communication to a PC. The Elegoo Uno R3 was programmed in the Arduino integrated development environment (IDE) to output the raw analog voltage readings from the analog-to-digital converter pin, displaying a number from 0 to 1023. These values were then mapped to a value between 0 to 5 Volts (V) within the IDE for means of mapping to the maximum voltage produced by the microcontroller. The real-time data was shown on the serial monitor of the IDE. Overall, for each line of data, the serial monitor would output the timestamp of the data taken, the raw voltage reading, and the raw voltage reading mapped to a value between 0 and 5V. The resulting data is in turn fed as an input into the ANN for classification after appropriate calculations.

Fig. 1. Panasonic AMN24112 PIR sensor with analog output capability.

Due to MI-PIR's close proximity to potential inanimate sources of heat, such as PCs, monitors, and printers, a thermal insulator was applied to limit local infrared radiation that might otherwise contaminate the voltage values and accuracy. The thermal insulator developed is made of cardboard, as part of the proof of concept stage of MI-PIR. Future work for long-term

Authorized licensed use limited to: OAKLAND UNIVERSITY. Downloaded on August 20,2020 at 14:47:54 UTC from IEEE Xplore. Restrictions apply.

deployment would to change the insulating material for greater longevity. The current design of the thermal insulator achieves this by simply covering the surrounding viewing angles of the MI-PIR sensor. The cardboard material was first experimented in the traditional deployment of a PIR sensor, and showed to be sufficient from blocking radiation from inanimate objects in motion.

The other half of the MI-PIR design comes with the robotic actuator that cycles the PIR sensor in a 130 degree motion. As a result, the overall horizontal detection range has been expanded with the novel MI-PIR design from 93 degrees to 223 degrees of coverage. The robotic actuator, Dynamixel MX-28, was previously programmed to scan in the forward direction (south to north) in 26 seconds and then back to the original position in 10 seconds, for an overall complete scan back to the original position in 36 seconds. This rotation has not been experimented with and has only been implemented for optimal usage in the lab. The Dynamixel MX-28 robot actuator holds a platform for the PIR sensor and thermal insulator; where, the platform provides no purpose other than to give the PIR sensor and the thermal insulator a flat surface to rest. The platform used in this work is a Hokuyo UTM-30LX-EW, which was used in a previous work. Fig. 2 displays the entire hardware setup for the MI-PIR design.

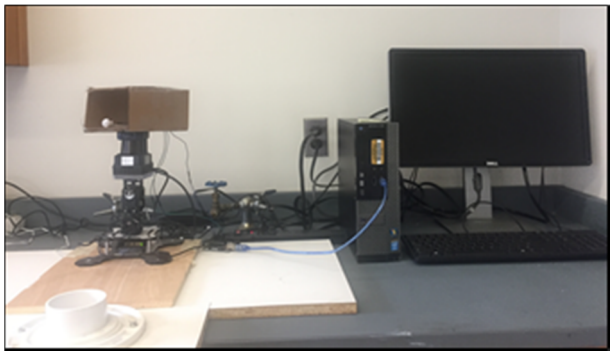

Fig. 2. Full MI-PIR Design.

B. Software

Deep learning is a powerful tool that is capable of achieving end-to-end learning from unstructured data. Given the robust nature, efficiency, and the lack of detailed feature extraction required, deep learning was an obvious choice for a problem as nonlinear as stationary human detection via PIR. The MI-PIR architecture primarily relies on an ANN in which a calculated version of the raw voltage data from the PIR is fed as an input, with the output being a classification of the current state of the room. The ANN models provide the ability to learn from the data and make accurate predictions that way. The ANN models are a set of algorithms that function similarly to a brain. The neural network associated the real-world data as numbers and make predictions based on the inputs [9].

Over the course of experimentation, four separate ANN models were developed for each of the four occupancy parameters, with each deviating slightly in terms of accuracy. Slight changes in architecture were applied for each of the ANN models as seen below in Table I. These modifications were necessary to deal with the number of output labels. Outside of these changes in output classification and architecture, the ANN models all received the same preprocessing for each of the experiments.

Table I. The four room occupancy parameters and the composition of their ANNs.

Occupancy Parameter	Optimizer	Output Activation	Loss	Layers (I, H, O)
Room Classification	sgd	sigmoid	binary_ crossentropy	2,2,1
Occupancy Count Estimation	adam	softmax	Sparse_ categorical_ crossentropy	16,16,4
Relative Location Prediction	adam	softmax	Sparse_ categorical_ crossentropy	128,128,32
Human Target Differentiation	adam	softmax	Sparse_ categorical_ crossentropy	128,128,32

The changes in optimizer, output activation function, loss calculation and layers were dependent on the task for each of these respective classification outputs. The room classification parameter has two states, either unoccupied or occupied, so as a result the binary_crossentropy loss function was used. Loss functions are used to measure the error between a network's output and a desired output. The room classification occupancy parameter used the stochastic gradient descent (sgd) optimizer while the other three room occupancy parameters used the adam optimizer. Optimizers are algorithms used to change the attributes of the neural network, such as weights and learning rate in order to reduce the losses [10]. The activation function is used to send "impulses" or map the output of the neuron to a certain value corresponding to a "yes or no". Finally, there are input (I), hidden (H), and output (O) layers that are individually given varying values that correspond to the number of inputs the ANN needs to process [11]. As a result, due to the fact that room classification has two labels, the ANN architecture follows a conventional binary classification model. As for the other three ANN models, each of them have more inputs and potential categories and are modified as such to match the task at hand.

The overall goal is to train the computer to learn the subtle variations in the continuous waveforms for classification purposes of the four different occupancy parameters: room classification, occupancy count estimation, relative location prediction, and human target differentiation. To meet that goal, data was preprocessed after collected from the Arduino IDE. The data was combined into one large CSV file with the Pandas concatenate function. Furthermore, the data was batched into 36 seconds based on the one complete cycle of the robotic actuator of MI-PIR, prepared for input via Numpy. After the data was separated into 36 second batches, the absolute value of the Fourier transform was calculated for each batch and used as the only feature for the ANN to learn from.

After trial and error with using standard deviation and raw voltage as the features to be learned from, the absolute value of the Fourier transform proved to be the most successful for learning. The absolute value of the Fourier transform batches

AFOSR grant FA9550-18-1-0287.

Authorized licensed use limited to: OAKLAND UNIVERSITY. Downloaded on August 20,2020 at 14:47:54 UTC from IEEE Xplore. Restrictions apply.

were normalized to be between 0 and 1 to aid in simplicity for the ANN. Finally, data was split between training, testing and validation at 70%, 15% and 15% respectively. Accuracies were obtained for each of the four room occupancy parameters with the results being analyzed and elaborated on in section V. Confusion matrices and F1-score values are presented in this section.

III. Experiments

For the purposes of testing MI-PIR in a closed indoor environment, an office space in an academic research building was used for data collection. This room is located in Dodge Hall of Oakland University and has five desk locations that have at least one PC and one monitor accompanying. Student researchers utilize these locations as work stations and the locations have variations in their subjects. All data collected with MI-PIR is during real working scenarios, with many of the subjects not knowing that they were actively being tested. This is important as to have normal movements during the day being collected, as a perfectly still subject for the length of time at the desk location is not a true indicator of a real-world application. There are six student researchers that are accounted for and labeled for during the data collection stage. Only those with a key access are allowed in the room.

There was a location in the room that need to be selected for optimal MI-PIR deployment. A desk location holds a PC, is a location that is not frequently used by any student researchers, and provides a higher vantage point than all other desk locations. In addition, this location provides the best scenario for a full scan of the room. These qualities made this location the optimal location for MI-PIR deployment. Fig.3 shows the view from this location at the vantage point of MI-PIR.

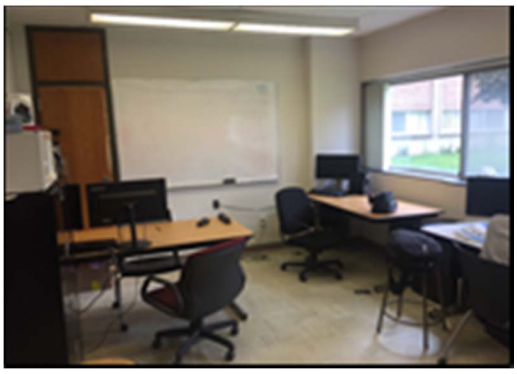

Fig. 3. The view from MI-PIR in Dodge Hall Room 120A.

For labeling purposes, the lab was segmented based on the desk locations. Fig. 4 lays out the lab in which data was collected, labeling the five various desk locations. Labels for deep learning purposes range from 0 to 25, where each of the number labels are associated with a location. When there are two people present, the smaller location number is presented first. For example, two people occupying the space at Locations 1 and 2 would be given a label of six, yet no label would be given for Locations 2 and 1 to avoid redundancy. MI-PIR is located at Location 1 in the office space. Locations 2 through 5 are consistently used as student work desks throughout data collection. There is variation between who is sitting at what location throughout the data collection process.

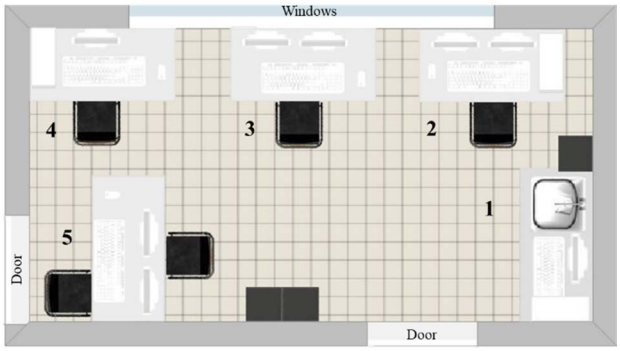

Fig. 4. Data labeling for the relative locations of human targets according to PC location. MI-PIR is at Location 1.

As data collected was taken normally as the student researchers worked, variations in the conditions exist. The blinds are open throughout much of the data collection process, allowing direct sunlight to enter in the office. However, in some datasets, the blinds were closed. Data was collected from 8/21/19 to 12/16/19, covering the changes in the seasons from the summer to winter months. Also during this time period, Location 3 lost an operating PC throughout the process. All of these changes provided varying ambient conditions. From varying sunlight, varying weather conditions, varying student researchers, and varying ambient heat in the room, the data collection process allowed for a wide range of datasets for the ANN to learn from. These changes make for a robust model, as all data collection was done under normal working conditions. The ANN learns from real-data and not under specific ambient conditions. Due to the varying environments, an ANN was the logical choice for determining differences in the data, as the voltages recorded from MI-PIR varied day to day.

Data was collected at a 10 Hz sampling rate. Data was only collected for occupied scenarios when the test subjects were sitting near a desk location or no one was in the office for an unoccupied state. All occupied data was collected with a constant student researcher being present, as this subject served as the ground truth in terms of data collection. Any change in state, such as a student researcher standing or moving from their desk location, would end that dataset and a new one would begin once all student researchers in the closed office space returned to a sitting position near or at their desk locations. In regards to an unoccupied state, ground truth for no student researchers present was administered by a student researcher outside the office door and verified by an OV7670 Arduino camera. This camera would take snapshots of the office door with five second durations and save them to the PC at Location 1. Scanning through the images would serve as a verification to the student user recording the room classification state in person.

Data was recorded in real-time from the Arduino IDE. The voltage output in the range of 0 to 1023 from the ADC pin of the analog PIR sensor was deleted and the 0 to 5 V range was saved and used. Labels of occupied or unoccupied, occupancy count, relative location prediction, and human target

Authorized licensed use limited to: OAKLAND UNIVERSITY. Downloaded on August 20,2020 at 14:47:54 UTC from IEEE Xplore. Restrictions apply.

differentiation were added manually. Integer labels are given for each occupancy parameter. These labels and the numbers associated from which the ANN will learn from are listed in Table II. Finally, the Excel sheet was converted into a CSV to be read by the ANN.

Table II. The labels used to indicate the different states associated with the closed office space.

Occupancy Parameter	Number Label	Real Label
Room Classification	0	Unoccupied
	1	Occupied
Occupancy Count Estimation	0	No People
	1	One Person
	2	Two People
	3	Three People
Relative Location Prediction	0	Unoccupied
	1	Location 1
	2	Location 2
	3	Location 3
	4	Location 4
	6	Locations 1 and 2
	10	Locations 2 and 3
	11	Locations 2 and 4
	12	Locations 2 and 5
	15	Locations 4 and 5
	23	Locations 2, 3, and 5
	24	Locations 3, 4, and 5
	25	Locations 2, 4, and 5
Human Target Differentiation	0	Unoccupied
	1	Student 1
	2	Students 1 and 2
	3	Students 1 and 3
	4	Students 1 and 4
	5	Students 1 and 5
	6	Students 1, 4, and 5
	7	Students 1, 3, and 5
	8	Students 1, 4, and 6

The timestamp was kept in a CSV file for the means of systematic data collection. Data was collected at the start of the cycle, where the robotic actuator ends the backward cycle and begins the forward cycle again. This process synced all the data at roughly the same time, allowing for the analysis of the data in terms of where the data collection began. During unoccupied states, 36 seconds would be added to the syncing timestamp to ensure enough time to leave the room. Although not always an exact syncing of data, this extra step allowed for a better chance of the ANN to learn from the data.

Overall, there are 3,657 batches of 36 second cycle datasets for the ANN. There are a total of 61 different scenarios that were collected during the data collection process, ranging from varying occupied and unoccupied scenarios. Some of the data conditions are less prevalent due to others. For example, organically collecting data for three stationary individuals is a greater challenge than collecting unoccupied data. Each of the data samples has a unique number of voltages as each sample was dependent on when the conditions changed. Two hours was the maximum time period of data collection, as the Arduino IDE serial monitor can only hold up to two hours of data at a 10 Hz sampling rate. The maximum conditions are for unoccupied states, whereas occupied conditions were dependent on human subjects sitting at their seat continuously.

IV. Data Analysis

The room classification occupancy parameter was labeled as 0 for unoccupied and 1 for occupied. In comparison of the two states visually, where voltage was on the y-axis from 0 to 5 V and time was the x-axis, there was a discernable difference. Visually, one can identify that occupied states have more heat recorded than unoccupied states during similar time frames on the same day; however, in comparison between unoccupied and occupied states between different days, the pattern was not upheld. An example of unoccupied and occupied states on the same day is shown in Fig. 5 and Fig. 6, respectively. This shows a discernable difference that provided the means of continuing the project forward. A threshold, however, could not be determined with signal processing or statistical methods alone. The signal processing techniques used in attempting to determine a threshold was the Fourier transform and Wavelet transform. Standard deviation, mean, and certain thresholds were trialed for the statistical methods. Due to the inability of these techniques to produce an adequate threshold between varying days, our attention turned to utilizing deep learning for this application.

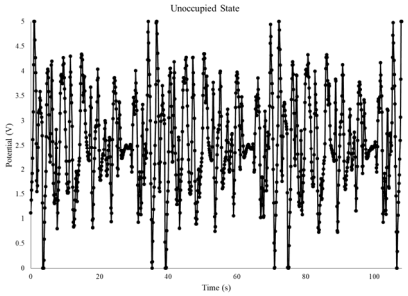

Fig. 5. An unoccupied office space.

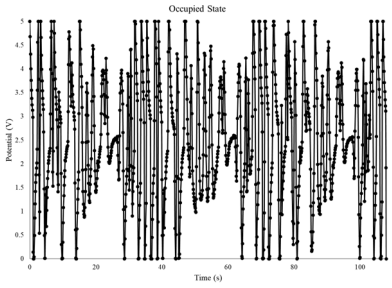

Fig. 6. An occupied office space.

Utilizing the raw voltage, as plotted in Fig. 5 and Fig. 6, the ANN produced low accuracy. Utilizing standard deviation as the feature inputted into the ANN, the ANN models again produced low results. Thus, the feature used for training in the ANN models was the minmax normalized absolute value of the Fourier transform of the raw PIR voltage data, in other words, the amplitude of the Fourier spectrum. This feature produced high accuracy for each of the four ANN models.

In identifying the accuracy presented from the ANN, the values in which the ANN learned from was plotted graphically

Authorized licensed use limited to: OAKLAND UNIVERSITY. Downloaded on August 20,2020 at 14:47:54 UTC from IEEE Xplore. Restrictions apply.

to identify the differences from which the ANN was able to learn. These figures were plotted using MATLAB. Fig. 7 though Fig. 10 identifies the discernable difference seen between the four different occupancy counts. Fig. 7 identifies the differences seen in the continuous waveforms between unoccupied and occupied states. The occupied state shows a higher amplitude than the unoccupied state across the data point range. The more people in the room, the greater the signal power was, as shown in Fig. 8 for the occupancy count estimation room parameter. Fig. 9 indicates the differences between Location 2 and Location 4 with the same student researcher present. Location 2 shows greater signal power than Location 4, overall. Location 2 is in closer proximity to Location 4, aligning with the PIR sensor theory that Location 2 would produce more signal power. Fig. 10 identifies the discernable differences seen between an occupancy state of student 1 and student 2 versus student 1 and student 3. Students 1 and 2 consistently shown higher signal power values than students 1 and 3. The amplitude of the Fourier spectrum is showed on the y-axis and the data points are plotted continuously on the x-axis for the following four figures.

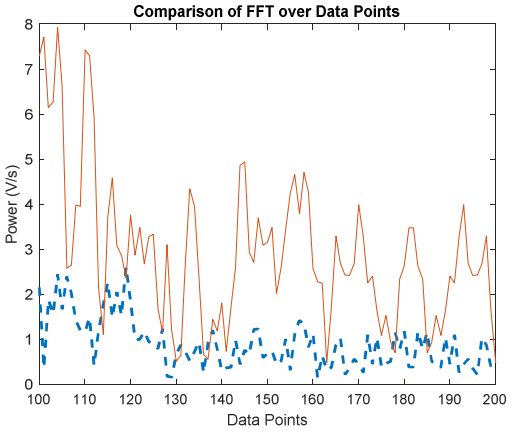

Fig. 7. Room classification state between unoccupied (blue/dashed) and occupied states (orange/solid).

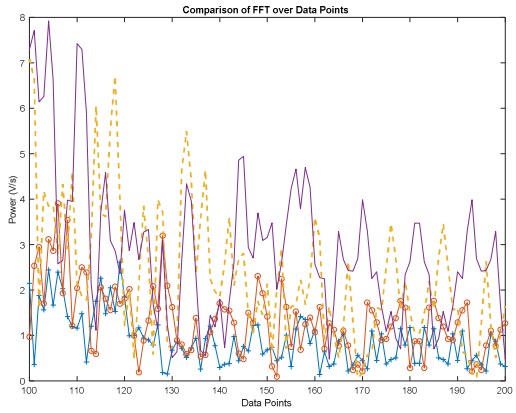

Fig. 8. Occupancy count estimation between no people (blue/dashed), one person (orange/circle), two people (yellow/dotted), and three people (purple/solid).

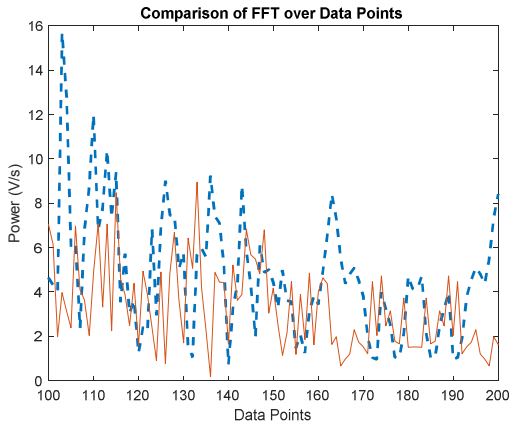

Fig. 9. Relative location prediction between Location 2 (blue/dotted) and Location 4 (orange/solid).

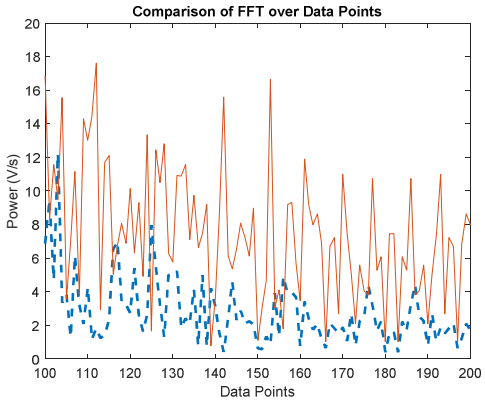

Fig. 10. Human target differentiation between Students 1 and 2 (orange/solid) and Students 1 and 3 (blue/dashed).

V. Results and Discussion

In classifying the occupancy state of a closed office space in an academic building, the ANN achieved an accuracy of 99%. For predicting the number of occupants present in a room, the ANN achieved an accuracy of 91%. In predicting the relative location of human targets in the closed office space, the ANN achieved an accuracy of 93%. Finally, in human target differentiation, the ANN achieved an accuracy of 93%. These accuracy results prove that the ANN was able to generate features through the waveforms from the absolute value of Fourier transform that was normalized to values between 0 and 1, to produce more accurate results with respect to the ground truth. This section aims to analyze the ANN performance parameters through output of confusion matrices, F1-score, precision and recall values.

Confusion matrices are used to gauge the performance of the data in terms of learning for the ANN. Confusion matrices serve the purpose as to identify true positive (TP), true negatives (TN), false positives (FP), and false negatives (FN) for learning from the dataset in question. TPs and TNs are the optimal result from the ANN, where the FP and FN indicate the percentage and number of batches that were not correctly classified. TPs and TNs are used to calculate precision and recall and he F1-score can be defined as the harmonic mean

Authorized licensed use limited to: OAKLAND UNIVERSITY. Downloaded on August 20,2020 at 14:47:54 UTC from IEEE Xplore. Restrictions apply.

between the precision and recall values. A perfect F1-score would be 1.0 while the lowest possible score is 0.0.

The occupancy classification of the closed office space produced the best results for our testing. Comparing between labels of 0 being unoccupied and 1 being occupied for stationary occupants, the ANN performed well in producing a high accuracy classification. Only discerning between two labels, room classification as unoccupied or occupied, the accuracy was reasonably the highest out of the four labels. A confusion matrix was produced with sklearn for the accuracy with a result shown below in Fig. 11. The F1 score, precision, recall are shown in Table III for the room classification parameter. Both of these graphical tools provide insight into the number of batches used for testing and the success of the ANN in comparing the occupied and unoccupied states.

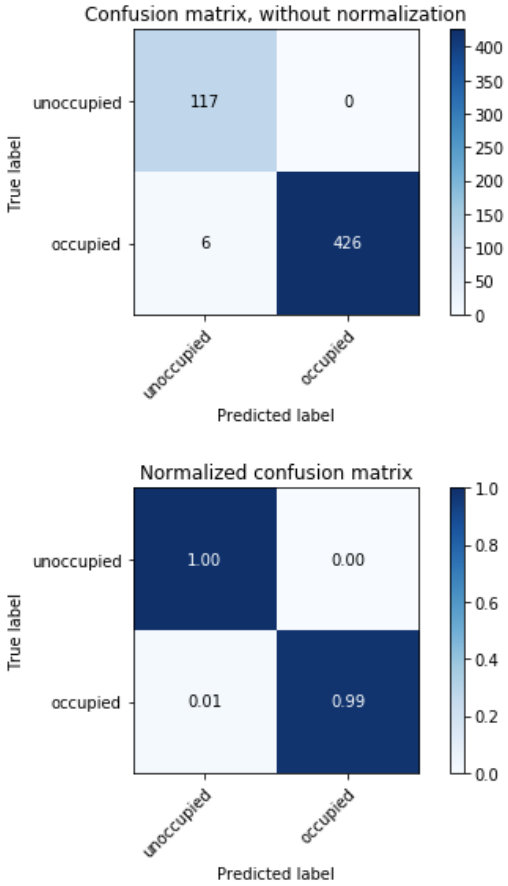

Fig. 11. Without normalization and normalized confusion matrices for room occupancy classification.

Table III. F1 score, precision, and recall for the room classification room occupancy parameter.

	Precision	Recall	F1-Score	Support
0	0.95	1.00	0.97	117
1	1.00	0.99	0.99	432
Accuracy			0.99	549
Macro Avg.	0.98	0.99	0.98	549
Weighted Avg.	0.99	0.99	0.99	549

There were 549 bacthes used for validation for each of the four occupancy parameters, with the number of occupied and unoccupied instances being randomly chosen for each. There were 426 batches for occupied and 117 batches for unoccupied. This is fifteen percent of the overall data. In addition, there were six batches that were misclassified, with the other 543 being corrrectly predicted. The six batches misclassified are considered FNs.

Each of the next three occupancy paramters will have accompanying confusion matrices and F1-score, precision, and recall tables. Fig. 12 and Table IVare for the occupancy count estimation parameter.

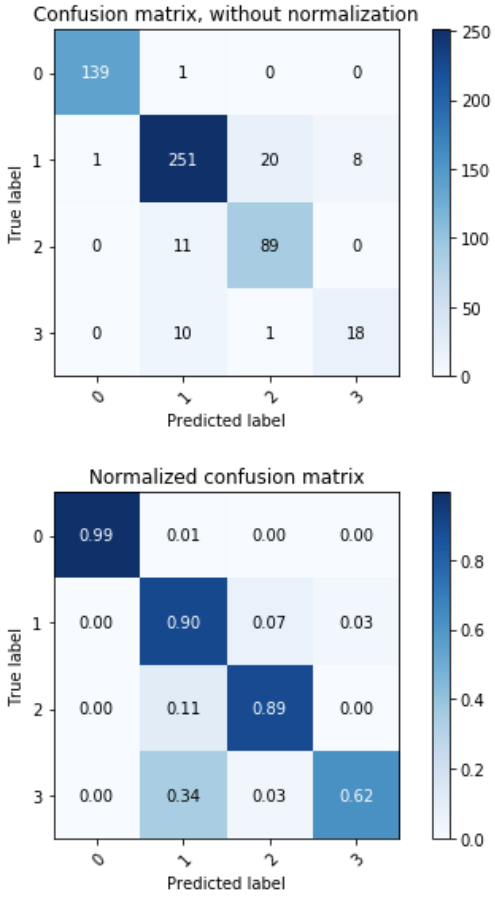

Fig. 12. Without normalization and normalized confusion matrices for occupancy count estimation.

Table IV. F1 score, precision, and recall for the occupancy count estimation parameter.

	Precision	Recall	F1-Score	Support
0	0.99	0.99	0.99	140
1	0.92	0.90	0.91	280
2	0.81	0.89	0.85	100
3	0.69	0.89	0.65	29
Accuracy			0.91	549
Macro Avg.	0.85	0.85	0.85	549
Weighted Avg.	0.91	0.91	0.91	549

Occupancy count estimation produced an overall accuracy of 91% for comparing the signal power of four different labels. Three people shows the worst accuracy out of the four labels, primarily due to the lack of data for this label. As shown in Table IV, the support for three people present is at 29 batches and the

Authorized licensed use limited to: OAKLAND UNIVERSITY. Downloaded on August 20,2020 at 14:47:54 UTC from IEEE Xplore. Restrictions apply.

next lowest is 100. Moreover, from examining the confusion matrix for this label, one can identify that there are discrepancies made with a prediction of 1 when in fact the correct label was 2 and 3, respectively. Based on the experiment design, a possible reason for this could be that the third person location collected was farther from MI-PIR at Location 5. Under further analyis of the occupancy count label of three people, we can see that the close proximity of Locations 3, 4, and 5 to eachother and the greater distance from MI-PIR may be added reasons for these errors. However, more data collection of three people, especially for instances where the third person is not located at Location 5, would be the most logical method to increase the accuracy for this occupancy parameter. Having the ANN model learn from the three people occupied label with varying locations would likely increase the results of this occupancy parameter.

Overall, MI-PIR was able to learn from the signal power waveforms and produce an accuracy of greater than 90% . Fig.13 and Table V are for the relative location prediction occupancy parameter.

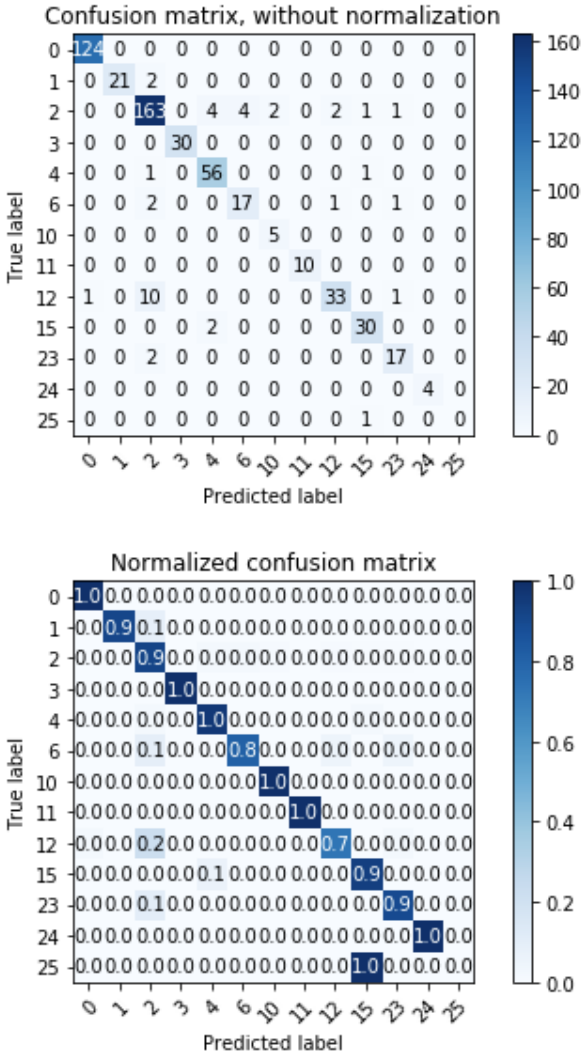

Fig. 13. Without normalization and normalized confusion matrices for relative location prediction.

Table V. F1 score, precision, and recall for the relative location occupancy parameter.

	Precision	Recall	F1-Score	Support
0	0.99	1.00	1.00	135
1	0.88	0.92	0.90	25
2	0.88	0.94	0.91	185
3	1.00	0.97	0.98	29
4	0.92	0.92	0.92	52
6	0.90	0.56	0.69	16
10	0.62	0.62	0.62	8
11	0.94	1.00	0.97	16
12	0.80	0.82	0.81	34
15	0.95	0.91	0.93	23
23	1.00	0.73	0.84	22
24	1.00	0.50	0.67	2
25	1.00	0.50	0.67	2
Accuracy			0.92	549
Macro Avg.	0.92	0.80	0.84	549
Weighted Avg.	0.92	0.92	0.92	549

Relative location prediction achieved an accuracy of 93%. From the confusion matrix, there is inaccuracies in the data mainly due to the relative lack of data. With more testing of certain examples, the ANN would theoretically perform better. The greatest challenges in accuracy are for the location labels which were similarly limited with respect to training data. In a controlled experiement, selecting the specific desk location combinations needed, the accuracy for these labels would likely increase. The selected instances of this data include labels of 10, 24, and 25. More data on these labels for training and testing would create a more balanced model and ultimately lead to higher accuracy.

Table 6 and Fig. 14 presented below are for the human target differentiation occupancy parameter. This occupancy parameter labels individuals from 0 to 8 for the inidividual subjects present in the office space. For example, a label of 0 corresponds to an unoccupied scenario, a label of 1 indicates “Subject A” present, and a label of 4 indicates “Subject A” and “Subject B” present. The inaccuracies in the data are centered around the lable of 1, with reason as this subject was present in each of the occupied scenarios.

Table VI. F1 score, precision, and recall for the human target differentiation occupancy parameter.

	Precision	Recall	F1-Score	Support
0	0.98	0.98	0.98	129
1	0.92	0.96	0.94	291
2	1.00	0.20	0.33	5
3	0.92	0.82	0.87	28
4	0.88	0.80	0.83	54
5	1.00	0.87	0.93	15
6	0.94	0.94	0.94	18
7	0.50	0.67	0.57	6
8	1.00	1.00	1.00	3
Accuracy			0.93	549
Macro Avg.	0.91	0.80	0.82	549
Weighted Avg.	0.93	0.93	0.93	549

Authorized licensed use limited to: OAKLAND UNIVERSITY. Downloaded on August 20,2020 at 14:47:54 UTC from IEEE Xplore. Restrictions apply.

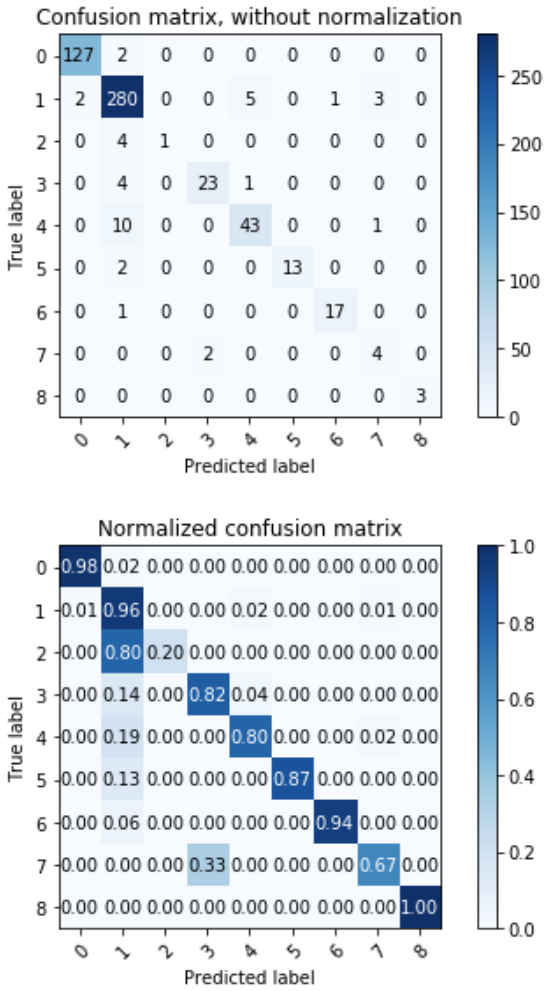

Fig. 14. Without normalization and normalized confusion matrices for human target differentiation.

Human target differentiation also obtained an overall accuracy of 93%. The greatest inaccuracies in the testing data, as evidenced in Table VI and Fig. 13, are the labels with the lowest amount of data, such as labels 2 and 6. Thus, with increased data collection for these labels, we would expect the accuracy to increase.

The ANN performed well at identifying the subtle variations between waveforms of varying types. ANNs are dependent on abundant training data, and with more data collected, the results are expected to increase. For most of the specific labels with lower accuracy results, the primary cause for their performance is the limited amount of data for these data samples. For example, limited data is available for three people occupying the office space in a stationary format at one time, due to the coordination of all individuals in a stationary set. This idea in comparison to unoccupied datasets that are easily recorded. More data collection will allow for unique samples to be better represented and accuracy to increase. All of the occupancy parameters are expected to improve with greater data collection in the areas of which there are limited samples of data available.

MI-PIR produced accurate results for all four occupancy parameters. MI-PIR produced an accuracy of 99% for room classification, whereas in [8] an accuracy of 97% was produced for their room classification experiment. The FoV is extended in this work from 93 degrees to 223 degrees, allowing for an entire office space in an academic building to be scanned and classified every 36 seconds. In motionless PIR sensors, the human subject in a space would have to be in the fixed FoV for detection. This system also detects stationary human targets with a simple design, while utilizing an ANN for classification and data processing. The most similar works, such as those in [6-8], rely on maximum sensing distance and room classification only. Through room classification, occupancy count estimation, relative location prediction, and human target differentiation, a single PIR sensor has shown expanded functionalities.

VI. Conclusions

MI-PIR is a novel approach to detecting stationary human targets in a closed space. With an accuracy of 99% for occupancy classification, 91% for number of people estimation, 93% accuracy for location estimation, and 93% for human target differentiation, MI-PIR shows accurate detection in a closed office space for all four of the occupancy parameters. MI-PIR extends the FoV of a traditional PIR sensor by 130 degrees, allowing for an entire office space to be scanned and classified every 36 seconds. MI-PIR allows for applications in a multitude of areas including energy management systems, surveillance, and alarm systems, amongst others. Passively detecting human targets allows for easier applications in real-world scenarios.

In future work, data collection of labels with limited number of samples would increase the accuracy results of this work. Further, reducing the power consumption from the Dynamixel MX-28 and improving the overall efficiency will be addressed. This could be addressed with a triggering of a traditional PIR sensor located at the door that starts the robotic actuator's movement. In future research, we plan to quantify the specs of MI-PIR. Specifically, including maximum distance of sensing and determining the optimal rotation pattern of the robotic actuator for performance. Identifying the maximum sensing distance for a stationary subject using MI-PIR would provide support that the FPs and FNs from the occupancy parameters are due to lack of data for select labels and not due to sensing distance. In addition, we intend on expanding MI-PIR's architecture to distinguish motion versus stationary states in the closed office space. The end goal would be to deploy MI-PIR for automated monitoring of a human subject by following their sleep and travel patterns.

Acknowledgment

This research is supported by AFOSR grant FA9550-18-1-0287 and the Bioengineering Summer Research Internship program at Oakland University.

References

[1] Gochoo, Munkhjargal & Tan, Tan-Hsu & Velusamy, Vijayalakshmi & Liu, Shing-Hong & Damdinsuren, Bayanduuren & Yeh, wei-chih. (2018).

Authorized licensed use limited to: OAKLAND UNIVERSITY. Downloaded on August 20,2020 at 14:47:54 UTC from IEEE Xplore. Restrictions apply.

Device-Free Non-Privacy Invasive Classification of Elderly Travel Patterns in A Smart House Using PIR Sensors and DCNN. IEEE Sensors Journal. 18. 390-400. 10.1109/JSEN.2017.2771287.

[2] Mokhtari, Ghassem & Zhang, Qing & Nourbakhsh, G. & Ball, Stephen & Karunanithi, Mohanraj. (2017). BLUESOUND: A New Resident Identification Sensor – Using Ultrasound Array and BLE Technology for Smart Home Platform. IEEE Sensors Journal. PP. 1-1. 10.1109/JSEN.2017.2647960.

[3] Akhter F, Khadivizand S, Siddiquei HR, Alahi MEE, Mukhopadhyay S. (2019). IoT Enabled Intelligent Sensor Node for Smart City: Pedestrian Counting and Ambient Monitoring. Sensors (Basel). 2019;19(15):3374.

[4] Kapu, Hemanth & Saraswat, Kavisha & Ozturk, Yusuf & Enis Cetin, A. (2017). Resting Heart Rate Estimation Using PIR Sensors. Infrared Physics & Technology. 85. 10.1016/j.infrared.2017.05.010.

[5] Hanosh, Ouday & Ansari, Rashid & Younis, Khaled & Cetin, A.Enis. (2019). Real-Time Epileptic Seizure Detection during Sleep using Passive Infrared (PIR) Sensors. IEEE Sensors Journal. PP. 1-1. 10.1109/JSEN.2019.2907664.

[6] Serfa Juan, Ronnie & Kim, Jin & Sa, Yui & Kim, Hi & Cha, Hyeong. (2016). Development of a Sensing Module for Standing and Moving Human Body Using a Shutter and PIR Sensor. International Journal of Multimedia and Ubiquitous Engineering. 11. 47-56. 10.14257/ijmue.2016.11.7.05.

[7] Wu, Libo & Wang, Y. & Liu, Haili. (2018). Occupancy Detection and Localization by Monitoring Nonlinear Energy Flow of a Shuttered Passive Infrared Sensor. IEEE Sensors Journal. PP. 1-1. 10.1109/JSEN.2018.2869555.

[8] Wu, Libo & Wang, Y. (2018). A Low Power Electric-Mechanical Driving Approach for True Occupancy Detection Using a Shuttered Passive Infrared Sensor. IEEE Sensors Journal. PP. 1-1. 10.1109/JSEN.2018.2875659.

[9] Nicholson, Chris. (2019). A Beginner's Guide to Important Topics in AI, Machine Learning, and Deep Learning. Pathmind. https://pathmind.com/wiki/neural-network

[10] Doshi, Sanket. (2019). Various Optimization Algorithms For Training Neural Network. Medium. https://medium.com/@sdoshi579/optimizers-for-training-neural-network-59450d71caf6.

[11] Ognjanovski, Gavril. (2019). Everything you need to know about Neural Networks and Backpropagation – Machine Learning Easy and Fun. Medium. https://towardsdatascience.com/everything-you-need-to-know-about-neural-networks-and-backpropagation-machine-learning-made-easy-e5285bc2be3a

[12] Bianco, Vittorio & Mazzeo, Pier Luigi & Paturzo, Melania & Distante, Cosimo & Ferraro, Pietro. (2020). Deep learning assisted portable IR active imaging sensor spots and identifies live humans through fire. Optics and Lasers in Engineering. 10.1016/j.optlaseng.2019.105818.

[13] Casaccia, Sara & Braccili, Eleonora & Scalise, Lorenzo & Revel, Gian. (2019). Experimental Assessment of Sleep-Related Parameters by Passive Infrared Sensors: Measurement Setup, Feature Extraction, and Uncertainty Analysis. Sensors. 19. 3773. 10.3390/s19173773.

[14] Gami, Hirenkumar. (2017). Movement Direction and Distance Classification Using a Single Pyroelectric IR Sensor. IEEE Sensors Letters. PP. 1-1. 10.1109/LSENS.2017.2782179.

[15] Hobson, Brodie & Lowcay, Daniel & Gunay, Burak & Ashouri, Araz & Newsham, Guy. (2019). Opportunistic occupancy-count estimation using sensor fusion: A case study. Building and Environment 159. 10.1016/j.buildenv.2019.05.032.

[16] Kim, Seonghyeon & Kang, Seokwoo & Ryu, Kwang & Song, Giltae. (2019). Real-time occupancy prediction in a large exhibition hall using deep learning approach. Energy and Buildings. 199. 10.1016/j.enbuild.2019.06.043.

[17] Li, Tianhong & Fan, Lijie & Zhao, Mingmin & Liu, Yingcheng & Katabi, Dina. (2019). Making the Invisible Visible: Action Recognition Through Walls and Occlusions.

[18] Mukhopadhyay, Bodhibrata & Srirangarajan, Seshan & Kar, Subrat. (2018). Modeling the Analog Response of Passive Infrared Sensor. Sensors and Actuators A Physical. 279. 65-74. 10.1016/j.sna.2018.05.002.

[19] Odat, Enas & Shamma, Jeff & Claudel, Christian. (2017). Vehicle Classification and Speed Estimation Using Combined Passive Infrared/Ultrasonic Sensors. IEEE Transactions on Intelligent Transportation Systems. PP. 1-14. 10.1109/TITS.2017.2727224.

[20] Pham, Minh & Yang, Dan & Sheng, Weihua. (2018). A Sensor Fusion Approach to Indoor Human Localization Based on Environmental and Wearable Sensors. IEEE Transactions on Automation Science and Engineering. PP. 1-12. 10.1109/TASE.2018.2874487.

[21] Singh, Saipriyati & Aksanli, Baris. (2019). Non-Intrusive Presence Detection and Position Tracking for Multiple People Using Low-Resolution Thermal Sensors. Journal of Sensor and Actuator Networks. 8. 40. 10.3390/jsan8030040.

[22] Yang, Tianye & Liu, Xuefeng & Tang, Shaojie & Niu, Jianwei & Guo, Peng. (2019). Push the Limit of PIR Sensor based Localization.

Authorized licensed use limited to: OAKLAND UNIVERSITY. Downloaded on August 20,2020 at 14:47:54 UTC from IEEE Xplore. Restrictions apply.